Compromised cardiovascular function in aged rats corresponds with increased expression and activity of calcium/calmodulin dependent protein kinase IIδ in aortic endothelium

Claire McCluskey, Laura Mooney[a], Andrew Paul and Susan Currie*

Strathclyde Institute of Pharmacy & Biomedical Sciences, University of Strathclyde, Glasgow G4 0RE

[a]current address: Nobel Biocare Services AG, P.O. Box 8058, Zurich-Airport, Switzerland

*Corresponding author

Tel: 00 44 141 548 2405 E-mail: susan.currie@strath.ac.uk

Abstract

Ageing is the greatest risk factor for cardiovascular disease. Calcium/calmodulin dependent protein kinase IIδ (CaMKIIδ) plays a fundamental role in the pathology of heart disease yet a potential role for CaMKIIδ in cardiovascular pathology associated with ageing remains unclear. Taking a combined *in vivo* and *in vitro* approach, we have for the first time investigated whether CaMKIIδ expression and CaMKII activity may be altered following age-related cardiovascular deterioration. Both cardiac contractility and aortic blood flow are compromised in aged rats and we have shown that this occurs in parallel with increased inflammation and crucially, autonomous activation of CaMKII. Endothelial cells isolated from young and aged aortae exhibit differences in cell phenotype and physiology. In line with observations in aortic tissue, aged aortic endothelial cells also show increased basal levels of pro-inflammatory markers and oxidative stress with concurrent increased basal activation of CaMKII. These results are the first to demonstrate that elevated CaMKIIδ expression and CaMKII activation occur in parallel with the pathological progression associated with ageing of the heart and vasculature. Specifically, CaMKIIδ expression is significantly increased and activated in the endothelium of aged aorta. As such, CaMKIIδ could serve as an important marker of endothelial dysfunction that accompanies the ageing process and may be an appropriate candidate for investigating targeted therapeutic intervention.

Key words: Ageing, Cardiovascular, Endothelium, Calcium/calmodulin protein kinase II, Inflammation, Oxidative stress

Abbreviations: CaMKII, calcium/calmodulin dependent protein kinase II; EC, endothelial cell; ED, endothelial dysfunction; ROS, reactive oxygen species; NFκB, nuclear factor kappa B

1. Introduction

Cardiovascular ageing is a complex and dynamic process involving not only changes to the heart muscle but also significant adaptations to the vasculature. A crucial feature of the aged vasculature is the development of endothelial dysfunction (ED), where a chronically 'activated' phenotype is adopted within the endothelium contributing to impaired vascular function [1]. Enhanced endothelial permeability and leukocyte adhesion is evident in the aged vasculature and it has been proposed that a chronic low grade inflammatory phenotype is evident in older people, significantly increasing the risk of illness and/or death [2]. The pathogenesis of ED associated with ageing is also mediated by reactive oxygen species (ROS). ROS, in particular superoxide (O_2^-) and hydrogen peroxide (H_2O_2), are known to be significantly elevated in aged individuals. They act to reduce the bioavailability of the endothelium-derived relaxing factor nitric oxide (NO), contributing to impaired endothelium dependent dilation (EDD) and this is often considered the first sign of adverse cardiovascular events [3,4]. ROS also play a role in activating various signal transduction pathways within vascular cells mediating the production of pro-inflammatory transcription factors such as Nuclear Factor kappa B (NF-κB) [2]. It is now generally accepted that both inflammation and oxidative stress work in parallel contributing to age-associated cardiovascular dysfunction. To date, there have been a variety of molecular mechanisms identified that may mediate endothelial dysfunction [5] however, the contribution of these pathways to both cardiac and vascular dysfunction remains uncertain.

Previous work has established that the multifunctional enzyme CaMKII is activated under conditions of increased oxidative stress (via methionine 281/282 oxidation) and inflammation in the heart [6,7]. CaMKII is encoded by four different genes (α, β, γ and δ) with CaMKIIδ being the major isoform expressed in heart. A direct link between the autonomously active enzyme and enhanced myocardial dysfunction has been well documented in numerous animal models of heart disease as well as in human hearts [8-10]. Indeed, such is the wealth of evidence for the pivotal role that CaMKIIδ plays in heart disease, there is growing confidence that targeting this enzyme could be an important advance in the treatment of heart disease [11-13]. It remains to be established whether CaMKII activation is observed during progressive cardiovascular dysfunction associated with ageing. Given the link between cardiac ageing and disease, this seems likely. It also seems possible that a similar relationship may exist in the vasculature however, much less is known of the role CaMKII plays in this environment. Several groups have reported that CaMKII signalling may contribute to vascular pathologies, such as atherosclerosis. This has primarily been shown in arterial smooth muscle cells (SMCs), where CaMKII has been identified as playing a key role in SMC proliferation, hypertrophy, migration and contraction [14-17]. It has been documented that both δ and γ isoforms of CaMKII are expressed in vascular smooth muscle and

endothelial cells [18]. However, more recently, studies in human umbilical vein endothelial cells have suggested that the δ isoform is prevalent in endothelium, specifically CaMKIIδ_6 [19]. This potential predominance of the δ isoform in the vascular endothelium is similar to what is observed in the heart. There is also some limited evidence that CaMKIIδ may be important in pathophysiological signalling in endothelial cells where modulation of endothelial nitric oxide synthase (eNOS) could also underlie CaMKIIδ contribution to atherogenesis [19,20]. However, currently nothing is known of whether endothelial CaMKII may exhibit sustained activation that could contribute to vascular dysfunction during the ageing process.

Here, we have taken both *in vivo* and *in vitro* approaches to compare the heart and vasculature (the aorta) between young and aged animals. We have assessed both heart and aorta function and have examined the status of CaMKII activation in both. We have confirmed both cardiac dysfunction and elevated blood flow in aged animals along with parallel increases in inflammation and oxidative stress. Importantly, and for the first time, we have shown that CaMKIIδ expression and CaMKII activation are increased in these hearts and CaMKII activation is also increased in aortae from aged animals. Specific focus on the vascular endothelium has demonstrated that an altered phenotype of endothelial cells isolated from the aged aortae corresponds with increased inflammatory status and oxidative stress as well as elevated CaMKIIδ expression and CaMKII activation in these cells. This work demonstrates for the first time a correlation between CaMKIIδ and the pathology accompanying not only the ageing heart, but also the ageing vasculature. Given what is already accepted about the principal role CaMKIIδ plays in diseased heart, the current work could serve as early evidence highlighting additional potential for this enzyme as a useful target for therapeutic intervention in the elderly population.

2. Materials and Methods

2.1 In vivo echocardiography

All procedures were performed under sterile conditions, complied with the ARRIVE guidelines and conformed to the *Guide for the Care and Use of Laboratory Animals* published by the US National Institutes of Health (NIH Publication No. 85-23, revised 1996) and Directive 2010/63/EU of the European Parliament. Male Sprague Dawley rats (young (10-12 week) and aged (18-20 month)) were briefly anaesthetised in a perspex chamber with 3% Isoflurane in the presence of 100% oxygen at a flow rate of 2L/min. After 2-3 minutes, rats were placed supine on a facemask and were maintained with 1.5-

2% Isoflurane in the presence of 0.5-1L/min oxygen. Fur was removed by application of a topical depilatory cream from the neck and upper chest area. For echocardiography of the heart, two-dimensional short axis views and M mode images were recorded at the level of the papillary muscle with the use of a MIUS HDI 3000CV echocardiography system, a 13MHz linear array transducer and ultrasound transmission gel. Systolic and diastolic LV wall measurements (including anterior wall (AW) and posterior wall (PW) measurements, LV end systolic dimension (LVESD), LV end diastolic dimension (LVEDD) and fractional shortening (%FS)) were assessed from M mode traces. Fractional shortening (FS) (%) is expressed as [LVEDD – LVESD/ LVEDD] x 100. An average of three measurements of each variable was used for each animal. For measurements of blood flow through the ascending aorta, a short axis view of the heart was obtained initially. The probe was then slowly turned ~70-80˚ clockwise to a longitudinal axis to allow a clear view of the vessels to be visualised. Brightness mode (B mode) ultrasound was used to measure vessel diameter and colour Doppler mode to visualise the direction of blood flow. Pulsed wave Doppler mode (PWD) was used to measure the velocity of blood passing through the ascending aorta. From these traces, the velocity time integral (VTI) and heart rate (HR) could be assessed. At least three measurements were recorded for velocity in the vessel per animal and an average taken. The blood flow was then calculated using the following formula:

$$Flow\ (ml/min) = VTI(Velocity\ Time\ Integral)\ x\ \pi r^2\ x\ HR\ (Heart\ Rate)$$

2.2 Preparation of cardiac and aortic homogenates

Hearts and aortae were dissected immediately following termination by intraperitoneal injection with pentobarbital sodium (10µl/g weight of animal; Euthatal) and heparin (0.1µl/g weight of animal; 5000 units/ml). Tissues were washed briefly in ice cold Ca^{2+}-free Krebs solution (120mM NaCl, 5.4mM KCl, 0.52mM NaH_2PO_4, 20mM Hepes, 11.1mM glucose, 3.5mM $MgCl_2$, 20mM taurine, 10mM creatine, pH 7.4). Cardiac ventricular tissue was finely minced on ice and whole tissue homogenates prepared as previously described [21]. Aortae were pulverised in liquid nitrogen using a mortar and pestle, until a fine white powder was formed. The frozen vessel was then solubilised by adding 10 volumes (W/V) of solubilisation buffer (50mM Tris pH 7.5, 50mM NaCl, 1% glycerol, 1mM EDTA, 1mM DTT, 1% Triton X, 1x protease inhibitors (Merck), 1 x phosphatase inhibitors (Merck)). This was left to mix end-over-end for 10 min at 4˚C before centrifugation at 13,000g for 5 min, also at 4˚C. The supernatant was then removed and used for subsequent experiments described below.

2.3 Isolation of rat aortic endothelial cells

The thoracic aorta was rapidly removed from rats following termination as described above. The vessel was flushed gently with warmed Ca^{2+}-free Krebs and any surrounding tissue was excised. A small clamp was used at one end of the vessel to close the opening of the lumen. Using a 19G needle, warmed Ca^{2+}-free Krebs solution containing 2mg/ml collagenase Type II (Worthington Chemicals, U.K.) was flushed inside the vessel. Another clamp was used to close the opening of the lumen at the opposite end, allowing only the inner endothelial lining of the aorta to be exposed to the enzyme for subsequent digestion. The collagenase-filled aorta was incubated for 10 min at 37˚C in an atmosphere of 5% CO_2. Following digestion, both clamps were removed and 5ml of culture media consisting of Dulbecco's Modified Eagle Medium (DMEM) supplemented with 20% (v/v) foetal calf serum (FCS), 1% (v/v), L-Glutamine and 2% Penicillin/ Streptomycin was added to the culture dish. Cells were separated by centrifugation at 1200g for 5 min before re-suspending the cell pellet in 5ml fresh culture media. This was then plated in a T25 flask and incubated at 37˚C in an atmosphere of 5% CO_2 for 4h. After this time, remaining smooth muscle cells and fibroblasts were removed by replacement with endothelial cell specific Medium G (20% FCS, 1000U/ml Penicillin-G, 100µg/ml Streptomycin, 2mM L-Glutamine, 1 x non-essential amino acids (GIBCO), 1 x sodium pyruvate (GIBCO), 25mM HEPES (pH 7 – 7.6, 100µg/ml heparin, 60µg/ml endothelial cell growth supplement (ECGS) (Sigma-Aldrich)) and endothelial cells grown to 60-80% confluency.

2.4 Haematoxylin and Eosin staining

Animals were euthanised as described above and aortae rapidly excised and washed thoroughly in ice cold Ca^{2+}-free Krebs solution. Tissue was fixed in 10% formaldehyde for 24h before being processed, embedded in paraffin wax and sectioned (5µm). Tissue sections were rehydrated then stained in haematoxylin for 6 min followed by eosin for 1 min. Slides were then dehydrated and mounted on coverslips before imaging. Five random sections per aorta sample and five areas of interest per sample were photographed at 10x magnification using a Leica DFC 320 camera (Leica Microsystems, Germany). Mean vessel width (µm) were then calculated from these images.

2.5 CD45 positive staining

Infiltration of leukocytes was assessed in fixed (10% formaldehyde), paraffin-embedded LV and aortic sections (5µm) with an anti-CD45 rat polyclonal antibody (1:250; BD BioSciences, Oxford, U.K.) using

diaminobenzidine (DAB) as the chromagen and Haematoxylin to counterstain. Five random sections per sample and five areas of interest per section were photographed at 40x magnification using a Leica DFC 320 camera (Leica Microsystems, Germany). Quantification was performed on Image J software, where the percentage of positive staining within a field of view was calculated.

2.6 TNF-α ELISA

Blood serum samples were collected from young and aged animals following cardiac puncture after euthanasia. Concentrations of TNF-α were determined using a commercially available ELISA kit following manufacturer's instructions (ELISA Ready-SET-Go! ®, eBioscience). Plates were read at 450nm using a BioTek EPOCH plate reader and Gen5 software. Standards were plotted using log-log linear fit and samples with absorbance readings falling within the linear range of the curve were quantified.

2.7 Detection of intracellular ROS

Young and aged cells were plated in a black-sided 96 well plate at 25,000 cells/well and allowed to attach overnight. Cells were then washed once with HBSS and stained with 25μM 2', 7'-dichlorofluorescein diacetate (DCFDA) (Abcam, Cambridge, MA) in HBSS for 45 minutes in the dark at 37°C. Cells were washed once with HBSS and treated with/without Ang-II for 3h in supplemented buffer (10% FCS (v/v) diluted in HBSS). 50μM Tert-Butyl Hydrogen peroxide (TBHP) was used as a positive control for the assay. Fluorescence was measured at 485nm excitation/535 emission.

2.8 CaMKII activity assay

CaMKII activity was assessed by measuring phosphorylation of a specific peptide substrate (autocamtide-2 (KKALRRQETVDAL)) by the transfer of γ phosphate of [γ-^{32}P]ATP by CaMKII. Assay components comprised Assay Dilution Buffer (ADB) (20mM MOPS, pH 7.2, 25mM β-glycerophosphate, 1mM Na_3VO_4, 1mM DTT, 1mM $CaCl_2$), Mg/ATP cocktail (75mM $MgCl_2$, 500μM ATP in 20mM MOPS, pH 7.2, 25mM β-glycerophosphate, 5mM EGTA, 1mM Na_3VO_4, 1mM DTT), CaMKII substrate cocktail (500μM autocamtide II (Merck) and 40μg/ml calmodulin in ADB) and PKA/PKC inhibitor cocktail (2μM PKA inhibitor peptide (Merck) and 2μM PKC inhibitor peptide (Merck) in ADB). Assay components were mixed on ice to a total volume of 40μl comprising 10μl ADB, 10μl substrate cocktail,

10µl inhibitor cocktail and 10µl CaMKII source (recombinant protein (Merck) or aorta homogenate) diluted to required concentration in ADB. Reactions were initiated by addition of 10µl [γ-^{32}P]ATP diluted to 1µCi/µl with Mg/ATP cocktail. Each sample was assayed in triplicate and incubated for 10 min at 30^{o}C with constant agitation. Following incubation, reactions were terminated by spotting 25µl on to P81 phosphocellulose paper. These were then washed in 0.75% phosphoric acid followed by acetone before counting in a scintillation counter. Specific radioactivity of the Mg/ATP cocktail was determined by counting 5µl directly and background counts were determined from samples in which the CaMKII source was absent.

2.9 Immunoblotting

Young and aged cells were grown on a 12-well plate 48h prior to assay and were solubilised with addition of 150µl 1x Laemmli buffer containing 75mM DTT. Samples were loaded onto 10% (v/v) acrylamide gels and analysed by SDS-PAGE using the BioRad® system. Following protein transfer to nitrocellulose, membranes were blocked in 5% (w/v) non-fat dry milk diluted in TBST buffer (20mM Tris-base, 137mM NaCl and 0.1% (v/v) Tween 20, pH 7.6) for 1h at room temperature. Membranes were then incubated overnight at 4˚C with antibodies against CaMKIIδ (rabbit polyclonal antibody 1:1000, custom-made against the C-terminus of CaMKIIδ (Eurogentec)), phosphorylated (phospho)-CaMKII (mouse monoclonal 1:500, Fisher Scientific) or oxidised (ox)-CaMKII (rabbit polyclonal 1:1000, GeneTex) prepared in 5% (w/v) BSA in TBST. Membranes were washed and then incubated for 2h at room temperature with either goat anti-mouse IgG-HRP (Sigma-Aldrich) or goat anti-rabbit IgG-HRP diluted 1:5,000 and 1:10,000 respectively. For quantitative analysis, following development membranes were stripped and re-probed for GAPDH expression as an internal loading control (mouse monoclonal 1:40,000 (Abcam). This was followed by addition of anti-mouse IgG-HRP (1:5,000). Scanned immunoblots were quantified by densitometry using a GS-800 densitometer and Quantity One Image software (version 4.5.2, BioRad) and signals expressed as ratios.

2.10 Immunofluorescence

Young and aged endothelial cells were grown on coverslips until confluent and fixed by aspirating the culture medium and applying ice cold methanol for 10 min. For experiments investigating phospho-NF-κB p65 (pp65) activation, young cells exposed to 10ng/ml TNFα (10 min) prior to fixation were used as a positive control. Cells were then washed 3 times with phosphate buffered saline (PBS) and permeabilised

with Triton X-100 (0.01% (v/v)) for 10 min. Non-specific binding was blocked using 1% (w/v) Bovine Serum Albumin (BSA) in PBS for 1h at room temperature followed by direct addition of primary antibody (CD31/Platelet endothelial cell adhesion molecule (PECAM)-1, 1:100; von Willebrand Factor (vWF), 1:100 (mouse monoclonal, Abcam); CaMKIIδ, 1:50; ox-CaMKII, 1:50 and pp65, 1:100 (rabbit polyclonal, Cell Signalling)), all prepared in 1% (w/v) BSA in sterile PBS and incubated overnight at 4˚C. Anti-rabbit IgG-TRITC and anti-mouse IgG-FITC conjugated secondary antibodies (Molecular Probes) were then applied at a 1:200 dilution for 1h at room temperature. After washing, coverslips were mounted using Mowiol® mounting medium containing DAPI (Vecta laboratory) and stored at 4˚C in the dark until they were viewed and photographed. The DAPI-counter stain in the mounting medium stained the cell nuclei blue. Pictures were taken using Nikon Eclipse^{TM} E600 Oil Immersion microscope connected to photometrics (CoolSnap^{TM} Fx) digital camera managed by MetaMorph^{TM} software (Universal Imaging Corporation, West Chester, PA).

2.11 Statistical Analysis

Data are expressed as mean ± SEM of *n* observations, where *n* represents the number of animals or samples. Statistical comparisons were performed using Student's unpaired *t* test, one- or two-way ANOVA followed by the appropriate post-test as indicated. Values of $p<0.05$ were considered statistically significant.

3. **Results**

3.1 In vivo measurements of cardiac and vascular function in young and aged rats

Short-axis views of the left ventricle in young and aged rats (Fig. 1A(i) and (iii)) were used to monitor cardiac contractility and M-mode traces (Fig. 1A(ii) and (iv)) measured to determine FS (%) for both age groups. There was a significant decrease in FS in aged animals when compared with young (Fig. 1B(i)) (63.2±1.3 vs. 50.6±1.9, young vs. aged, p=0.005, n=8) indicating compromised contractile function in aged hearts. In line with the observed decrease in FS, there was also a significant decrease in heart rate (HR) (bpm) in aged animals (Fig. 1B(ii)) (334±13 vs. 271±6, young vs. aged, p=0.006, n=11). Furthermore, there was a significant increase in heart size reflected as increased heart weight:body weight ratio (HW/BW) in the aged group (2.68±0.2 vs. 3.63±0.1, young vs. aged, p=0.04, n=11).

As well as cardiac dysfunction, ageing is associated with vascular dysfunction. Fig. 2A shows the functional changes in aortic blood flow that accompany ageing. Long axis views of young and aged

aortae are shown in Fig 2A (i) and (ii) respectively. PWD was used to measure the speed with which the pressure wave travels along the vessel. Overall, blood flow (ml/min) was faster in aged vessels (velocity peaks are higher as shown in Fig. 2A(iv) compared with young vessels (Fig. 2A (iii)) (76.7±4 vs. 104±9.7, young vs. aged, p=0.05, n=9) and there was more turbulence, reflected in the spread of normalised flow measurements (Fig. 2A(v)). In line with altered blood flow, the physiology of the aorta was also altered in aged animals. The overall size and lumen of the vessel was larger in aged animals (Fig. 2B(i)) and aged vessels showed increased medial wall thickness (16.4±0.9 vs. 28±1.5 (μm), young vs. aged, p=0.003, n=9) (Fig. 2B(ii)).

3.2 Quantification of CaMKIIδ expression and CaMKII activation in heart and aorta of young and aged animals

Following in vivo echocardiographic assessment of cardiovascular function, cardiac and aortic tissue from aged animals were processed for immunoblotting as described in the methods section. As shown in Fig 3A(i) and (ii) CaMKIIδ expression was significantly increased in aged heart ((CaMKIIδ:GAPDH)1.03±0.04 vs. 1.71±0.26, young vs. aged, p=0.03, n=7). Using site-specific antibodies generated against the phospho-Thr 286/287 site and the ox-Met 281/282 site on CaMKII, expression levels of both 'activated' forms of the enzyme were measured in young and aged hearts. Levels of phospho-CaMKII were significantly increased in aged hearts ((pCaMKII:GAPDH) 0.85±0.09 vs. 1.19±0.12, young vs. aged, p=0.04, n=7) as were levels of ox-CaMKII ((oxCaMKII:GAPDH) 0.9±0.08 vs. 1.14±0.04, young vs. aged (heart), p=0.03, n=5). Fig 3B (i) and (ii) show the results from similar experiments conducted for young and aged aortae. There was no significant difference in CaMKIIδ expression observed in the aged aorta (1.03±0.07 vs. 1.26±0.1, young vs. aged, p=0.09, n=7), however upon examining each of the variants (individual bands) shown in the blot (Fig. 3B(i)) there appeared to be a greater increase in certain variants over others in the aged aorta. A true reflection may only come from analysing each variant separately. Levels of both phospho-CaMKII and ox-CaMKII were significantly increased in aged aortae compared with young, (pCaMKII:GAPDH)1.16±0.13 vs. 1.82±0.2, young vs. aged, p=0.04, n=7 and (oxCaMKII:GAPDH) 1.02±0.01 vs. 1.3±0.07, young vs. aged, p=0.01, n=4). To investigate CaMKII activity in aged aorta using an alternative approach, aortic homogenates were used as a source of CaMKII to measure incorporation of [^{32}P]ATP into autocamtide II (a CaMKII-specific peptide substrate) in the presence of PKA and PKC inhibition. Fig 4A shows the specificity of the kinase assay using recombinant(r) CaMKIIδ. Fig 4A(i) shows total ^{32}P measured for each treatment and Fig 4A(ii) specific activity following each treatment where 10ng and 30ng of rCaMKIIδ resulted in

activity levels of ~200pmol phosphate incorporated into the autocamtide peptide substrate/min/μg protein. When the assay is performed with rCaMKIIδ in the absence of substrate or in the absence of $CaCl_2$, activity levels fall to close to zero. When the assay is performed without rCaMKIIδ, activity is also close to zero. Using the same assay to assess tissue preparations, Fig 4B shows that CaMKII activity associated with aortic homogenates from young animals showed no significant difference compared with control whereas, activity associated with aged aortae was increased significantly relative to control ((pmol PO_4^-inc/min) 2.31±0.56 (control no enzyme), 5.95±1.9 (young, p=0.054, n=3), 8.21±1.4 (aged, p=0.03, n=3) and this supports the evidence for increased CaMKII activity in aged aortae as assessed by phosphorylation and oxidation of CaMKII shown in Fig. 3.

3.3 Measurement of inflammatory markers in young and aged rats

Initial data examining circulating inflammatory molecules showed that levels of TNFα were increased in the blood of aged animals when compared with young ((pg/ml) 0.002±0.002 vs. 22.05±12.9, young vs. aged, p=0.02, n=4) (Fig. 5A). There was considerable spread in the aged data, reflecting the labile nature of TNFα and variation across animals. N numbers were low due to availability of blood samples for animals in the current study therefore further experiments sought to investigate whether evidence for leukocyte infiltration into aged tissues (presumably in response to increased cytokine levels) may be apparent in aged heart and aortae. Sections of heart and aorta were examined for expression of CD45 as an indicator of leukocyte infiltration. Fig 5B (i) and (ii) show CD45 staining in representative sections of left ventricular tissue from young and aged animals respectively and quantification is shown in Fig 5B (iii) reflecting an increase in staining in aged heart ((% CD45 positive cells) 3.25±0.2 vs. 14.87±1.7, young vs. aged p=0.006, n=6). Fig. 5C (i) and (ii) shows CD45 staining in representative sections of aorta from young and aged animals respectively. Fig. 5C (iii) shows the quantification analysis reflecting an elevation in CD45 staining in the aortae of aged animals when compared with young but without a significant increase ((%CD45 positive cells) 3.02±0.9 vs. 9.7±2.4, young vs. aged p=0.08, n=6).

3.4 Phenotypic alterations in aortic endothelial cells isolated from young and aged aortae

Having established that aged aortae exhibit significant changes functionally and physiologically and that this correlates with a significant increase in CaMKIIδ expression and activation, it was of interest to examine this link at the level of the endothelium. Initially, it was important to establish that alterations at the level of the aorta were replicated in the endothelial cells (ECs) of these vessels. ECs were isolated

from young and aged aortae as described in the methods section. A modified technique (outlined in the methods section) was used to obtain high purity yields of cells and resultant cultures were stained for both von Willebrand factor (vWF) and PECAM-1 (Fig. 6A). The isolation technique provided EC cultures of >95% purity. Cells were isolated from young and aged aortae and kept in culture for up to 8 days with growth rate and cell phenotype monitored. Fig 6B shows typical images obtained from both (i) young and (ii) aged aortic ECs from day 2 until day 8 post-isolation. Cell growth rate was slower for aged cells (cell numbers were consistently fewer following eight days in culture for aged versus young cells) and the characteristic EC shape was lost with cells appearing larger, more rounded and stressed (red circles show representative cells exhibiting this phenotype). There also appeared to be dark granules or vacuoles in the cytoplasm and around the nucleus of aged cells (yellow arrows indicate these granules). Since these were not examined in detail, it is difficult to predict what they represent however, it is likely that they are associated with cell damage.

3.5 Measurement of pro-inflammatory signalling and oxidative stress in aortic endothelial cells from young and aged aorta

Phosphorylation (activation) of the pro-inflammatory mediator NFκB sub-unit (phospho-p65) was monitored in ECs isolated from each either young or aged aortae. Results are shown in Fig. 7A(i) where there is a clear increase in the basal phospho-p65 signal in aged cells in the absence of any external stimulus. In young cells, there is no obvious basal signal for phospho-p65 (i.e. no obvious inflammatory status). To investigate this further, cells from young animals (where there is no basal signal for phospho-p65) were stimulated with TNFα for 10 min prior to staining. There was a significant increase in phospho-p65 signal following TNFα stimulation of young cells, reflecting the potential for activation of this pathway in these cells. Interestingly, the levels of phospho-p65 in young cells following stimulation were almost equivalent to levels observed in aged cells without any stimulation ((signal intensity/cell) 4.75±0.2 vs 22.45±1.3, young vs. aged, $p=0.007$, $n=3$ and 4.75±0.2 vs. 23.52±1.1, young vs. young TNFα stimulated, $p=0.006$, $n=3$) (Fig 7A(ii)). As an additional measure of the stressed phenotype of the aged ECs, levels of intracellular ROS were measured and compared in young and aged cells (Fig. 7B). Cell permeant DCFDA was used to assess intracellular ROS activity as outlined in the methods section. DCFDA is converted to a highly fluorescent compound dichlorofluorescein upon oxidation and can therefore be used to quantify total intracellular ROS activity as a fluorescent signal generated in cells where ROS activity is present. Under basal conditions, aged ECs had significantly higher levels of intracellular ROS than young cells (1556±365 vs. 4065±915 (a.u.), young vs. aged, $p=0.03$, $n=3$). To

verify that the DCFDA assay could detect changes in intracellular ROS production upon stimulation of cells, both groups of cells were also treated with 10μM angiotensin II (AngII) for 3h. As would be expected, in response to stimulation both young and aged groups showed increased levels of intracellular ROS and, interestingly, aged cells still produced significantly higher levels than young cells, reflecting what is observed under basal conditions (4856±2754 vs. 8047±2095 (a.u.), young vs. aged, p=0.04, n=3).

3.6 Comparison of CaMKIIδ expression and oxidation in endothelial cells from young and aged aorta

ECs isolated from young and aged aortae were assessed for CaMKIIδ expression and, given the elevated levels of ROS observed in cells from the aged group, for levels of 'activated' ox-CaMKII. Immunofluorescence experiments showed that both CaMKIIδ (Fig. 8A(i)) and ox-CaMKII (Fig. 8A(ii)) were highly expressed under basal conditions in aged cells but there was little, if any, staining evident in cells isolated from young aortae. To measure CaMKIIδ and ox-CaMKII in cell populations from both young and aged groups, quantitative immunoblotting was used. Interestingly, and in agreement with the immunofluorescence data, expression levels of both total CaMKIIδ (Fig. 8B(i)) and ox-CaMKII (Fig. 8B(ii)) were significantly increased in aged cells when compared with young ((CaMKIIδ:GAPDH) 0.98±0.14 vs. 1.92±0.33, young vs. aged, p=0.04, n=4 and (ox-CaMKII:GAPDH) 0.85±0.06 vs. 1.13±0.02, young vs. aged, p=0.007, n=4).

4. Discussion

The present study is the first to show that CaMKIIδ expression and autonomous CaMKII activation are elevated in the heart and the vasculature (aorta) of aged animals. Crucially, this study examined CaMKII in parallel with functional output and inflammatory status of these animals. There was evidence for significant cardiac and vascular remodelling and compromised function as well as increased inflammation as would be anticipated in the aged animal. Specific examination of aortic ECs showed that CaMKIIδ expression and oxidised CaMKII were both significantly elevated in aged samples. Importantly, these CaMKII measurements were performed in parallel with phenotypic assessment and inflammatory status of the aged cells. It is well known that ED is pivotal to the vascular dysfunction that accompanies ageing and disease. We have confirmed that aged cells exhibit a stressed phenotype, have elevated pro-inflammatory signalling and have significantly higher levels of intracellular ROS. In the presence of elevated oxidative stress, it is not surprising that CaMKII is oxidised and activated, leading to a myriad of pathological effects on the aged vessel.

A number of parallels between the aged cardiovascular system and young diseased cardiovascular system have already been observed and although ageing itself doesn't necessarily cause heart failure, there is a greater propensity for cardiovascular disease to manifest [22]. It is known that the heart becomes stiffer with age as there is increased deposition of fibrous tissue and fat. Cardiac output (CO) declines and results in a less efficient response to increased workload. The decrease we observed in the HR of aged animals likely reflects physiological changes occurring at the level of the sino-atrial node where there may be cell loss and/or dysfunction. Since HR is one of the key factors contributing to CO and with ageing there is a reduction in CO, it is not surprising to observe a decline in HR in our aged animals. The elevation we observed in blood flow in aged vessels correlates with previous work where aortofemoral pulse wave velocity was shown to increase with age and to be a predictor of future cardiovascular events [22].

Findings from the present study provide strong support for CaMKIIδ playing a multi-faceted role throughout the cardiovascular system during progression of ageing-induced pathology, and suggest CaMKIIδ may not just be a molecular switch for the heart but also for the vasculature in aged individuals. Previous work has shown that vascular injury in vivo results in up-regulation of CaMKIIδ in vascular smooth muscle (VSM) cells in the medial layer [17]. Indeed, there is significant evidence to suggest that elevated CaMKIIδ promotes a synthetic VSM phenotype and regulates proliferation and motility, leading to vascular wall remodelling [23]. More recent work has shown that the oxidised form of CaMKII is elevated in vivo after vascular injury and in VSM cells following in vitro treatment with agonists that are known to increase levels of intracellular ROS [24]. In addition to effects on the VSM cells, CaMKII has also been shown to contribute to pathophysiological signalling in ECs [19]. However, as far as we are aware, there are no reports to date of the role that CaMKIIδ may play in mediating ED associated with ageing.

The endothelium of the cardiovascular system, although only a single cell layer thick, exhibits an extraordinary capacity for modulation of cardiovascular function. It is clear that, like many cell types in vivo, the endothelium cannot be viewed as a homogeneous population of cells. In vivo, ECs are continually subjected to shear stress from blood flow and this is likely to be different within different branches of the vascular tree and will differ according to the health of the individual. Indeed, as we have shown in the present study, flow can alter according to age and it is likely that ECs will adapt not only to disturbances related to age or disease, but will also adapt to changes along the vascular tree in healthy conditions. This may involve changing cell phenotype and alterations in protein expression to accommodate the environment [25]. We recognise that cultured ECs do not exactly mimic the in vivo situation since they are studied under static conditions without any resident neighbouring VSM cells and

may present with a different phenotype from what would be observed in vivo. The key point for the present study though is that both groups of ECs (young and aged) have been treated identically yet still exhibit significant physiological and biochemical differences and crucially, what we observe in the intact aortic tissue (in terms of CaMKIIδ expression and activation) is mirrored in the isolated aortic ECs. Interestingly, we observe more significant changes in CaMKIIδ and ox-CaMKII in aged ECs when compared with aged aortic tissue. This may reflect the importance of CaMKII in modulation of aged EC function although we have not compared with possible changes to CaMKII in other cell types of the vasculature in these aged animals.

It is worth noting that a recent study has provided evidence for increased agonist-evoked endothelial calcium signalling in aged carotid arteries [26]. The authors describe this as somewhat of a paradox in a situation where decreased endothelial function and eNOS activity is seen. There is an analogy between this data and what has been shown in the present study. Increased calcium signalling in the aged endothelium could lead to increased CaMKII activation and sustained autonomous CaMKII activity. As we know from a wealth of studies in cardiac myocytes, elevated CaMKII activity is only useful up to a certain point. There must be a fine balance and control over the switch from basal to sustained activation and pathological consequences. This rule could also hold true for the vascular endothelium, where there may be potential for increased calcium signalling in aged animals leading to increased CaMKII activation and ultimately vascular dysfunction.

Although we refer to the endothelium as though it were a homogeneous entity, we know this is not the case. It is essential that the complexity and heterogeneity of the endothelium is not forgotten, particularly in the context of the present study. How apt that a molecule often referred to as a molecular switch in the heart, should prove to be significantly switched on in aged aorta, and even more so in aged endothelium. CaMKIIδ could serve as an immediate transducer of altered calcium handling along the entire body of the endothelium, switching rapidly between resting and activated status in regions of greater stress. It is also pertinent that CaMKII sensitivity is increased in damaged and aged VSM cells [27]. Altered CaMKII signalling could play a crucial role in the communication between VSM cells and ECs and as such, could impact significantly on the dysfunction observed at the level of both cell types during ageing.

There is still much that remains unknown regarding the mechanisms that underlie cardiovascular dysfunction associated with ageing. What is clear from the present study is that CaMKII (a molecule we know to be central to cardiac health and disease [28] is activated in synchrony with pro-inflammatory pathways and oxidative stress in the aged cardiovasculature. It seems likely that up-regulation and

activation of CaMKII will contribute to ED and in that sense, its pathological actions are likely to mirror those observed in the contractile cells of the diseased heart [29].

5. Conclusion

This study confirms that CaMKII activity and expression of the CaMKIIδ isoform are up-regulated in both aged heart and aged aortae. This occurs in parallel with deterioration of cardiovascular function. Specific examination of endothelial cells isolated from aged aortae confirms that CaMKII is oxidised and activated in line with an increased inflammatory and oxidative stress status in these cells. Future work should focus on determining the effects of selective inhibition of CaMKIIδ in the aged endothelium. This will be essential for our understanding of how CaMKII may contribute to the local heterogeneous as well as to the global more homogeneous, responses of the endothelium in the aged animal. It will also be important to decipher the potential for different delta variants playing specific roles in cellular and sub-cellular function. With a wealth of increasing evidence now supporting a vital role for CaMKII in both cardiac and vascular dysfunction at the level of numerous resident cell types, the argument for therapeutics designed towards specific modulation of cardiovascular CaMKII to combat functional deficits becomes progressively more convincing.

Acknowledgements We would like to thank Margaret MacDonald and Graeme McKenzie for their expert technical assistance with echocardiography and Adrian Thompson (University of Edinburgh) for his expertise in pulsed wave Doppler imaging. This work was supported by the BBSRC (grant no: BBSRC DTG Bb/F017642/1).

Ethical approval All applicable international, national and institutional guidelines for the care and use of animals were followed.

Conflict of interest The authors declare they have no conflict of interest.

References

[1] Deanfield, J.E., Halcox, J.P., Rabelink, T.J. (2007) Endothelial function and dysfunction: testing and clinical relevance. Circulation 115, 1285-1295

[2] Csiszar, A., Wang, M., Lakatta, E.G., Ungvari, Z. (2008) Inflammation and endothelial dysfunction during ageing: role of NFκB. J.Appl.Physiol. 105, 1333-1341

[3] Li, T., Chen, Y., Gua, C., Li, X. (2017) Elevated circulating trimethylamine N-oxide levels contribute to endothelial dysfunction in aged rats through vascular inflammation and oxidative stress. Front. Physiol. 8, 350

[4] Yoon, H.J., Cho, S.W., Ahn, B.W., Yang, S.Y. (2010) Alterations in the activity and expression of endothelial NO synthase in aged endothelial cells. Mech.Ageing.Devpt. 131, 119-123

[5] Laina A., Stellos K., Stamatelopoulos K. (2018) Vascular ageing: underlying mechanisms and clinical implications. Exptl.Gerontol. 109, 16-30

[6] Erickson J.R., Joiner M.A., Guan X., Kutschke W., Yang J., Oddis C.V. et al. (2008) A dynamic pathway for the calcium-independent activation of CaMKII by methionine oxidation. Cell 133, 462-474

[7] Singh M.V., Swaminathan P.D., Luczak E.D., Kutschke W., Weiss R.M., Anderson M.E. (2012) MyD88 mediated inflammatory signalling leads to CaMKII oxidation, cardiac hypertrophy and death after myocardial infarction. J.Mol.Cell.Cardiol. 52, 1135-1142

[8] Backs, J., Backs, T., Neef, S., Kreussner, M.M., Lehmann, L.H., Patrick, D.M., et al. (2009) The delta isoform of CaM kinase II is required for pathological hypertrophy and remodelling after pressure overload. Proc Natl Acad Sci USA 106, 2342-2347

[9] Colomer, J.M., Mao, L., Rockman, H.A., Means, A.R. (2003) Pressure overload selectively up-regulates Ca^{2+}/calmodulin-deoendent protein kinase II in vivo. Mol.Endocrinol. 17, 183-192

[10] Sossalla, S., Fluschnik, N., Schotola, H., Ort, K.R., Neef, S., Schulte, T., et al. (2010) Inhibition of elevated CaMKII improves contractility in human failing myocardium. Circ.Res. 107, 1150-1161

[11] Zhang R., Khoo M.S., Wu Y., Yang Y., Grueter C.E., Ni G. et al. (2005) CaMKII inhibition protects against structural heart disease. Nat. Med. 11, 409-417

[12] Banyasz, T., Szentandrassy, N., Toth, A., Nanasy, P.P., Magyar, J., Chen-Izu, Y. (2011) Cardiac calmodulin kinase: a potential target for drug design. Curr.Med.Chem. 18, 3707-3713

[13] Currie, S., Elliott E.B., Smith G.L., Loughrey C.M. (2011) Two candidates at the heart of dysfunction: the ryanodine receptor and calcium/calmodulin protein kinase II as potential targets for therapeutic intervention – an in vivo perspective. Pharmacol. Ther. 131, 204-220

[14] Zhu L.J., Klutho P.J., Scott J.A., Xie L., Luczak E.D., Dibbern M.E. et al (2014) Oxidative activation of CaMKII regulates vascular smooth muscle cell migration and apoptosis. Neurochem.Int. 67, 1-8

[15] Maione, A.S., Cipolletta, E., Sorriento, D., Borriello, F., Soprano, M., Rusciano, M.R. et al. (2017) Cellular subtype expression and activation of CaMKII regulate the fate of the atherosclerotic plaque. Atherosclerosis 256, 53-61

[16] Marganski, W.A., Gangopadhyay, S.S., Je, H.D., Gallant, C., Morgan, K.G. (2005) Targeting of a novel CaMKII is essential for extracellular signal-regulated kinase mediated signalling in differentiated smooth muscle cells. Circ. Res. 97, 541-549

[17] Singer, H., 2012. CaMKII function in vascular remodelling. J. Physiol. 590,1349-1356

[18] Cai, H., Liu, D., Garcia, J.G.N. (2008) CaM Kinase II-dependent pathophysiological signalling in endothelial cells. Cardiovasc. Res. 77, 30-34

[19] Wang, Z., Ginnan, R., Abdullaev, I.F., Trebak, M., Vincent, P.A., Singer, H.A. (2010) CaMKII delta 6 and RhoA involvement in thrombin-induced endothelial barrier dysfunction. J. Biol. Chem. 285, 21303-21312

[20] Murthy S., Koval O.M., Ramiro Diaz J.M., Kumar S., Nuno D., Scott J.A. et al. (2017) Endothelial CaMKII as a regulator of eNOS activity and NO-mediated vasoreactivity. PLOS ONE 12(10):e0186311

[21] Martin, T.P., Robinson, E., Harvey, A., Grieve, D.J., MacDonald, M., Paul, A. et al. (2012) Characterisation and optimisation of a minimally invasive aortic banding procedure to induce cardiac hypertrophy. Exptl. Physiol. 97, 822-832

[22] Strait, J.B., Lakatta, E.G. (2012) Ageing-associated cardiovascular changes and their relationship to heart failure. Heart. Fail. Clin. 8, 143-164

[23] House, S.J., Ginnan, R.G., Armstrong, S.E., Singer, H.A. (2007) CaMKIIδ isoform regulation of vascular smooth muscle cell proliferation. Am. J. Physiol. Cell. Physiol. 292, C2276-C2287

[24] Scott, J.A., Xie, L., Li, H., Li, W., He, J.B., Sanders, P.N. et al. (2012) The multifunctional Ca^{2+}/calmodulin-dependent kinase II regulates vascular smooth muscle migration through matrix metalloproteinase 9. Am. J. Physiol. Heart. Circ. Physiol. 302, H1953-H1964

[25] Potter, C.M.F., Lundberg, M.H., Harrington, L.S., Warboys, C.M., Warner, T.D., Berson, R.E. et al. (2011) Role of shear stress in endothelial cell morphology and expression of cyclooxygenase isoforms. Arterioscler. Thromb. Vasc. Biol. 31, 384-391

[26] Wilson, C., Saunter, C.D., Girkin, J.M., McCarron, J.G. (2017) Advancing age decreases pressure-sensitive modulation of calcium signalling in the endothelium of intact and pressurised arteries. J.Vasc. Res. 53, 358-369

[27] Lundberg, M.S., Crow, M.T. (1999) Age-related changes in the signalling and function of vascular smooth muscle cells. Exptl.Gerontol. 34, 549-557

[28] Feng, N., Anderson, M.E., 2017. CaMKII is a nodal signal for multiple programmed cell death pathways in heart. J. Mol. Cell. Cardiol. 103, 102-109

[29] Zhang, T., Brown, J.H., 2004. Role of CaMKII in cardiac hypertrophy and heart failure. Cardiovasc. Res. 63, 476-486

Figure Legends

Fig. 1 Cardiac hypertrophy and contractile dysfunction is evident in aged rats. (**A**) Representative ultrasound of a two-dimensional short axis view of the heart obtained in (i) young and (iii) aged rats. Visualisation of structures including the left ventricle (LV), anterior wall (AW), posterior wall (PW) and the papillary muscles (PM) were obtained. M mode traces were recorded at the level of the PM and are shown for (ii) young and (iv) aged animals respectively. These were used to generate systolic and diastolic wall measurements: LV end systolic dimension (LVESD) and LV end diastolic dimension (LVEDD). Images are representative of n=8 (young) and n=11 (aged) rats. (**B**) Scatter plots representing mean fractional shortening (%) and heart rate values (bpm) in young and aged animals, n=8 for young and n=11 for aged rats. (**C**) Histogram showing mean heart weight:body weight (HW:BW) for young and aged rats, n=10 for each group. All data are expressed as mean ± S.E.M and data analysed using a student's unpaired t test, *$p<0.05$, **$p<0.01$.

Fig. 2 Blood flow and aortic physiology is altered in aged animals. (**A**) Representative parasternal long axis (PLAX) view of the ascending aorta (AA) obtained in (i) young and (ii) aged rats using ultrasound to show LV and aortic valve (AV) structures. For assessing blood flow, a Pulsed Wave Doppler mode was used where blood velocity traces could be visualised in (iii) young and (iv) aged animals. All images are representative of n=9 for both young and aged rats. (v) Blood flow (ml/min) through the AA was calculated using the formula described in the methods section. All values were normalised to AA diameter, n=9 for both groups. (**B**) Histological representation of aortae dissected from young and aged rats by H&E staining. The left hand panel shows a section taken from the aorta of a young animal and the right hand panel shows a section taken from an aged counterpart. Images are representative of n=3 for both groups at 10x magnification (scale bar shown is 500µm). (ii) Histogram showing mean aorta wall

thickness in young and aged rats. Values are plotted as mean ± S.E.M and data analysed using a student's unpaired t-test, n=3, **p<0.01.

Fig. 3 CaMKIIδ expression and activation via phosphorylation and oxidation are increased in aged heart and aortae. (**A(i)**) Representative immunoblots of total CaMKIIδ, phosphoThr286/7 (p)-CaMKII and oxMet281/282 (ox)-CaMKII expression in young and aged rat whole heart homogenates (10μg loads total protein) are shown in addition to expression of the loading control GAPDH. (**ii**) Densitometry analysis was performed and data normalised to GAPDH for each immunoblot. Mean normalised data are shown in accompanying histograms for CaMKIIδ n=7, p-CaMKII n=7 and ox-CaMKII n=5, *p<0.05. (**B(i)**) Representative immunoblots of CaMKIIδ, phosphoThr286/7-CaMKII and oxMet281/282 (ox)-CaMKII (10μg total protein loads) are shown for young and aged whole aortic homogenates together with (**ii**) histograms displaying mean normalised data ± S.E.M. for CaMKIIδ n=7, p-CaMKII n=7, and ox-CaMKII. Statistical analysis was performed using a student's unpaired t-test, n=4,*p<0.05.

Fig. 4 Basal CaMKII activity is significantly increased in aortae from aged animals. (**A**) Histogram showing assay specificity with activity obtained from 10ng and 30ng recombinant CaMKIIδ in **(i)** counts per minute (cpm) as well as **(ii)** phosphate incorporated into specific autocamtide II peptide substrate/min /μg protein. Activity was monitored in the presence of inhibitors to PKA and PKC and in the presence and absence of autocamtide substrate (w/o substrate), in the presence or absence of $CaCl_2$ (w/o Ca^{2+}) and in the absence of rCaMKII (w/o CaMKII). Data are from one experiment, representative of two others. (**B**) Histogram showing CaMKII activity (using the same assay) in young and aged whole aortic homogenates (10μg total protein) when compared with background activity (no source of enzyme). Activity was measured as [^{32}P] incorporated into specific autocamtide II peptide substrate/min/10μg protein. Data are expressed as mean ± S.E.M,. Statistical analysis was performed using a two-way ANOVA and Tukey's post-test, n=3, *p<0.05.

Fig. 5 Increased serum TNFα levels and leukocyte infiltration of cardiovascular tissues are evident in aged animals. (**A**) TNF-α ELISA analysis of terminal sera samples taken from young and aged rats. Values are plotted as mean ± S.E.M, n=3 for young; n=4 for aged groups, *p<0.05. (**B**) Positive CD45 staining in LV cardiac sections from (i) young and (ii) aged rats with (iii) histogram showing quantification (% CD45 positive cells). (**C**) Positive CD45 staining in aortic tissue from (i) young and (ii) aged rats with (iii) histogram showing quantification (% CD45 positive cells) in aorta. Images are shown

of each tissue at 40x magnification, and are representative of n=6 for both groups (scale bar = 100μm). Data was analysed using a student's unpaired t test; n=6 for both groups, $p<0.01$**.

Fig. 6 Endothelial cells isolated from aged aortae show altered phenotype. (**A**) Endothelial cells were successfully isolated from adult rat aorta and characterised by (i) PECAM-1 and (ii) v-WF staining. Panels (iii) and (iv) show positive staining of HUVECs for both markers respectively (positive controls). Panels (v) and (vi) show aortic endothelial cells stained with anti-rabbit or anti-mouse IgG-FITC secondary antibody alone respectively (negative control for both stains). (**B**) Representative images of aortic endothelial cells isolated from (i) young and (ii) aged rats and grown in culture for up to eight days (10x magnification). Images are representative of n=3 experiments, all at 10x magnification.

Fig. 7 Pro-inflammatory signalling and oxidative stress are both significantly elevated in aged endothelial cells. (**A**(i)) Staining for basal phospho-p65 expression in young and aged aortic endothelial cells. TNFα -stimulated young aortic endothelial cells served as a positive control. Where appropriate, cells were stimulated with TNFα (10ng/ml) for 10 min. Images are representative of n=3 for each condition and are shown at 10x magnification. (**A**(ii)) Quantification of pp65 signal intensity/cell was performed and data analysed using a one-way ANOVA followed by Tukey's post-test; n=3 for each group; $p<0.01$**. (**B**) Histogram showing intracellular ROS production in young and aged endothelial cells with and without 10μM Ang-II (3h) stimulation. Young cells treated with 50μM TBHP (3h) served as a positive control for the assay. All data are expressed as mean (a.u.) ± S.E.M. Statistical analysis was performed using a one-way ANOVA and Tukey's post-test, n=3 *$p<0.05$.

Fig. 8 CaMKIIδ and ox-CaMKII expression are increased in aged aortic endothelial cells. (**A**) Representative images of young and aged endothelial cells stained for (i) total CaMKIIδ and (ii) ox-CaMKII. Cells stained with secondary anti-rabbit IgG TRITC-conjugated antibody alone served as a negative control. Images are representative of n=3 experiments, all at 10x magnification (scale 100μm). (**B**) Immunoblot analysis of (i) CaMKIIδ and (ii) ox-CaMKII expression in young and aged aortic endothelial cells (~10^4 total cells). Data was normalised to intrinsic GAPDH expression and plotted as mean ± S.E.M in accompanying histograms, Data was analysed using a student's unpaired t-test, n=4, *$p<0.05$, **$p<0.01$.

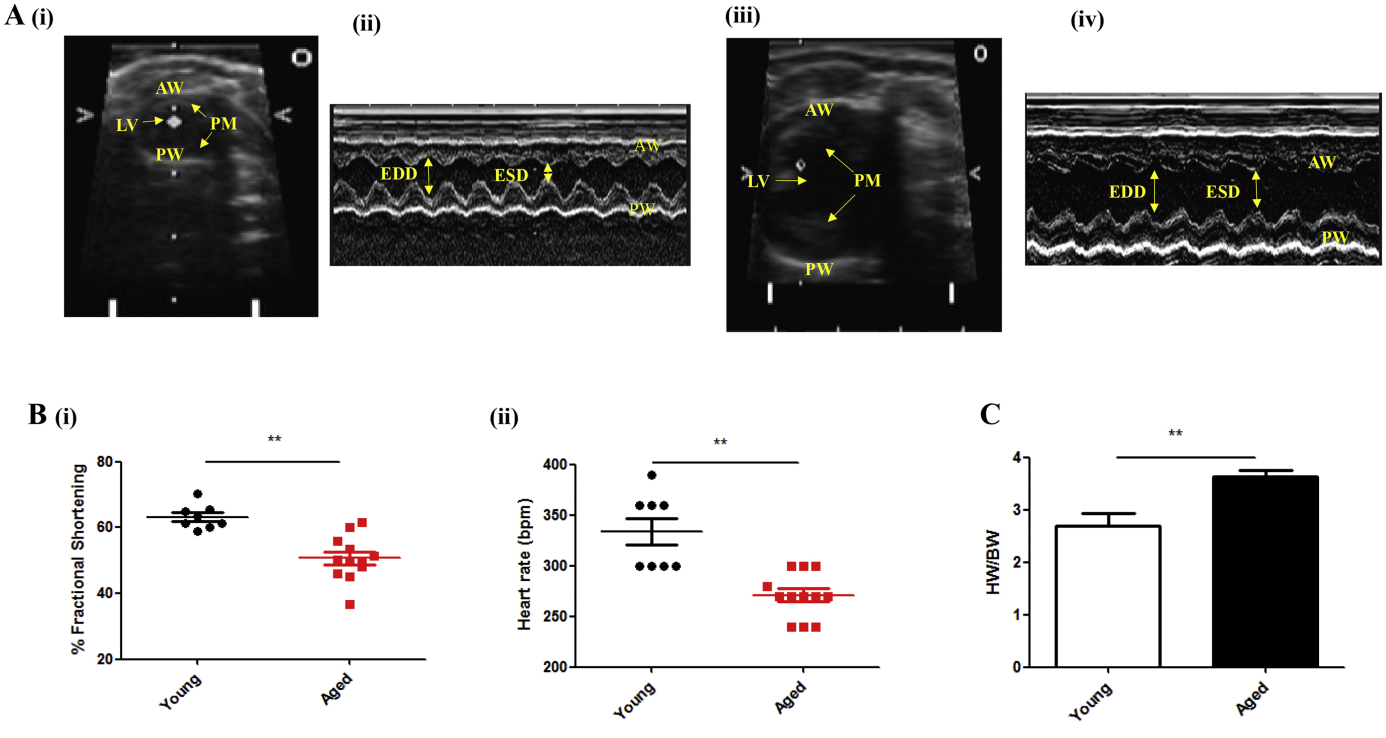
A (i)
(ii)
(iii)
(iv)
AW
LV
PM
PW
EDD
ESD
B (i)
% Fractional Shortening
80
60
40
20
**
Young
Aged
(ii)
Heart rate (bpm)
400
350
300
250
200
C
HW/BW
4
3
2
1
0

Figure 1

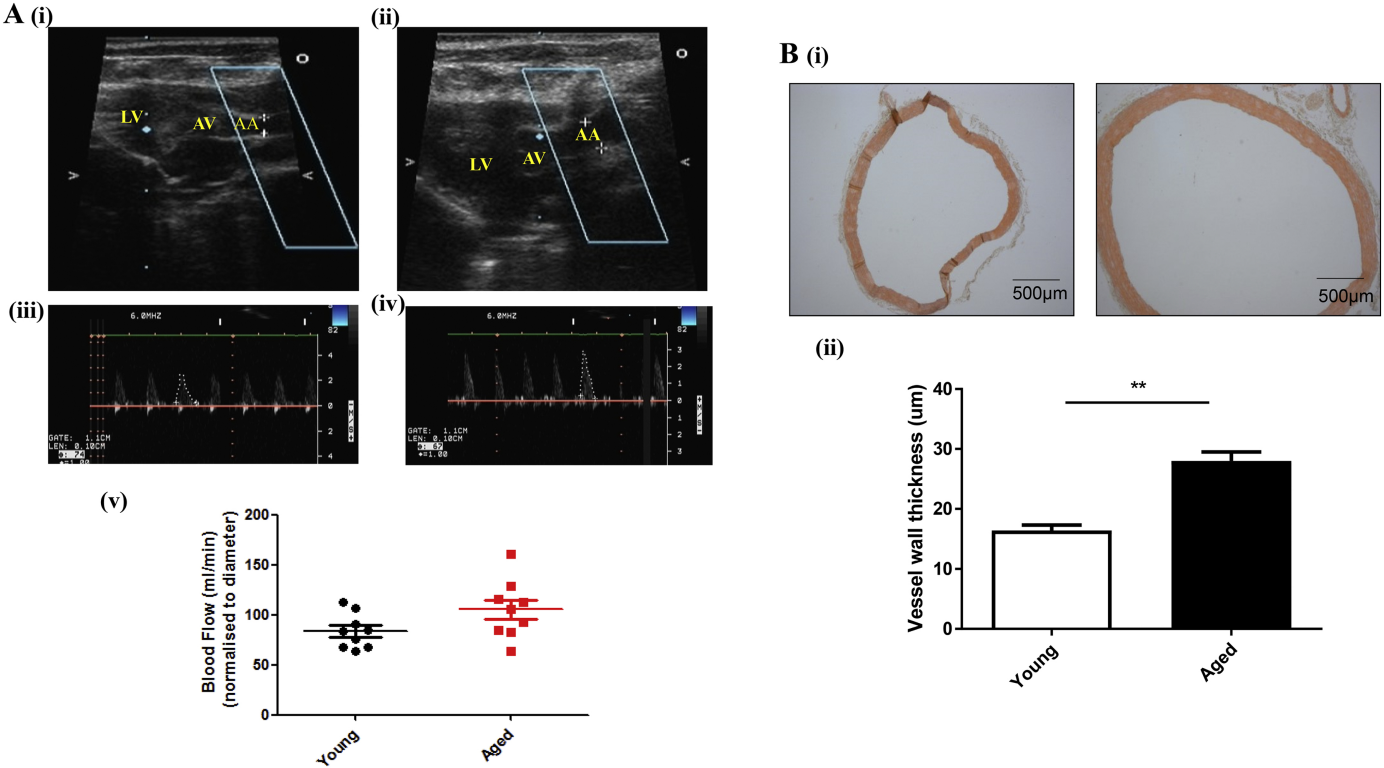
A (i)
(ii)
LV
AV
AA
(iii)
(iv)
6.0MHZ
(v)
Blood Flow (ml/min)
(normalised to diameter)
200
150
100
50
0
Young
Aged
B (i)
500µm
500µm
(ii)
Vessel wall thickness (um)
40
30
20
10
0
**
Young
Aged

Figure 2

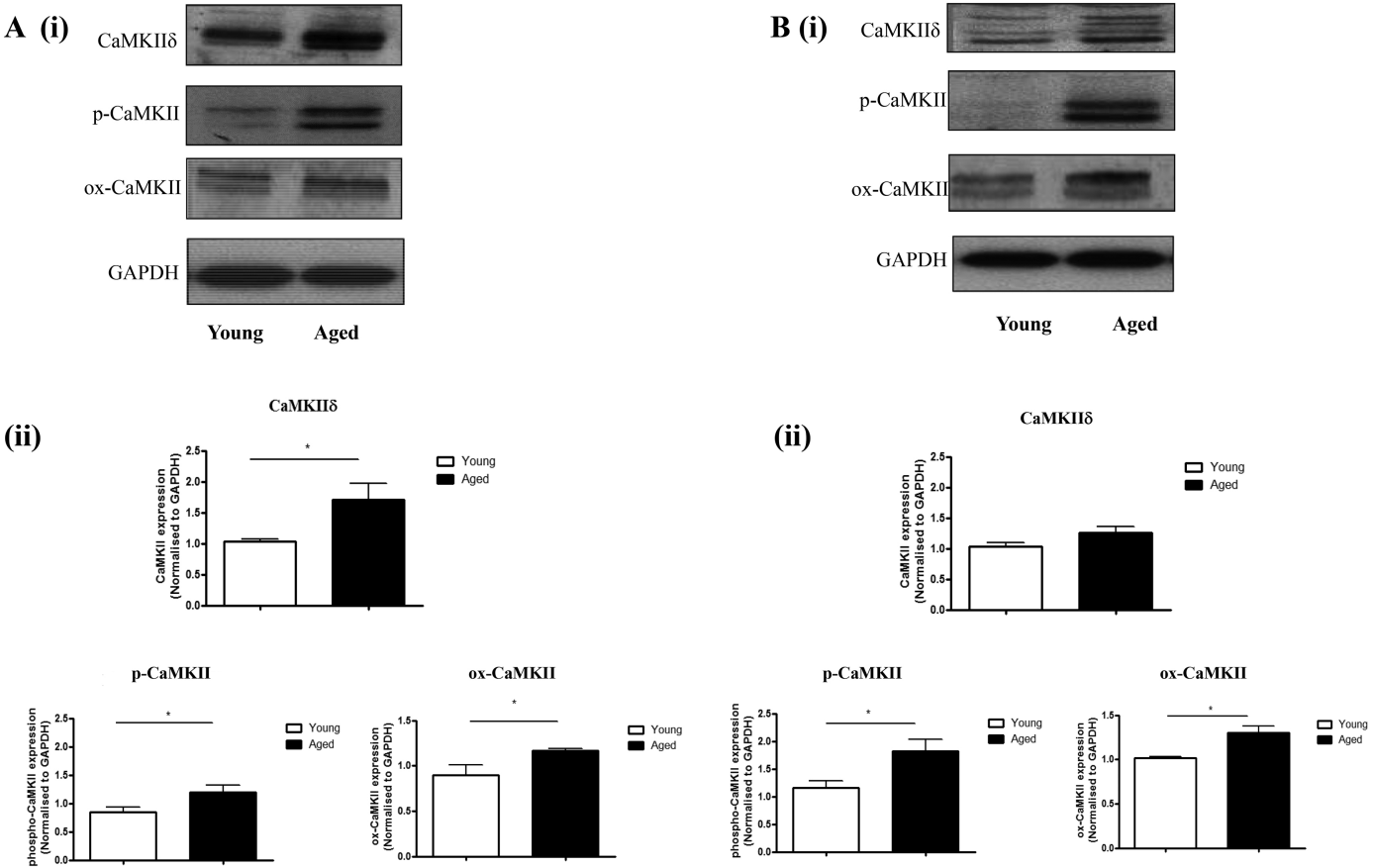
A (i)
CaMKIIδ
p-CaMKII
ox-CaMKII
GAPDH
Young
Aged
B (i)
CaMKIIδ
p-CaMKII
ox-CaMKII
GAPDH
Young
Aged
(ii)
CaMKIIδ
CaMKII expression (Normalised to GAPDH)
Young
Aged
p-CaMKII
phospho-CaMKII expression (Normalised to GAPDH)
ox-CaMKII
ox-CaMKII expression (Normalised to GAPDH)
(ii)
CaMKIIδ
CaMKII expression (Normalised to GAPDH)
p-CaMKII
phospho-CaMKII expression (Normalised to GAPDH)
ox-CaMKII
ox-CaMKII expression (Normalised to GAPDH)

Figure 3

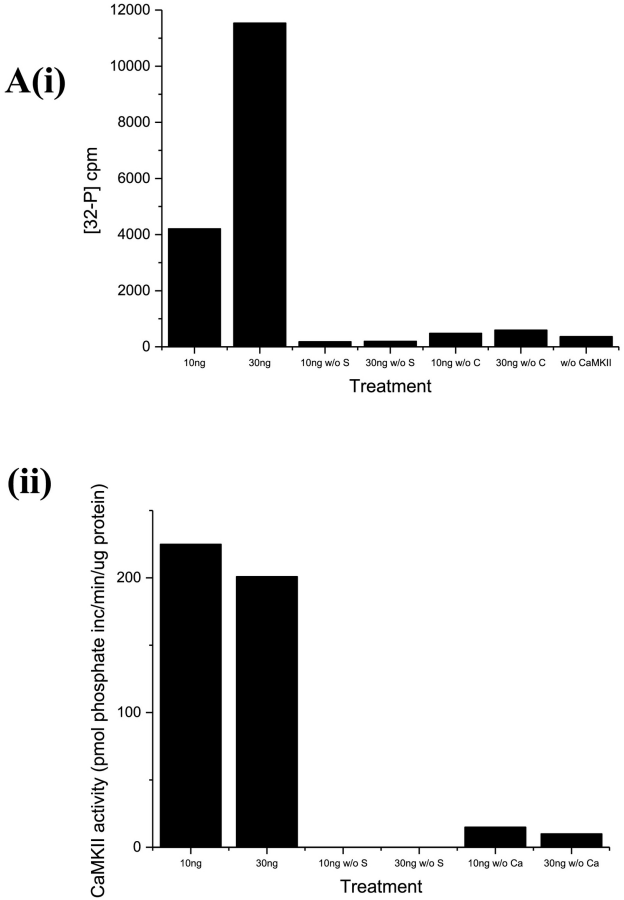
A(i)
12000
10000
8000
6000
4000
2000
0
[32-P] cpm
10ng
30ng
10ng w/o S
30ng w/o S
10ng w/o C
30ng w/o C
w/o CaMKII
Treatment
(ii)
CaMKII activity (pmol phosphate inc/min/ug protein)
200
100
0
10ng
30ng
10ng w/o S
30ng w/o S
10ng w/o Ca
30ng w/o Ca
Treatment
B
*
ns
CaMKII activity
(pmol PO4 incorp. per 10µg protein)
10
8
6
4
2
0
No enzyme
Young aortae (10ug)
Aged aortae (10ug)

Figure 4

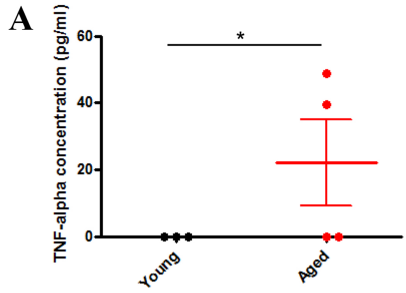
A
TNF-alpha concentration (pg/ml)
60
40
20
0
*
Young
Aged

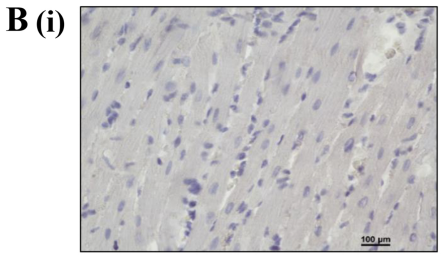
B (i)
100 µm

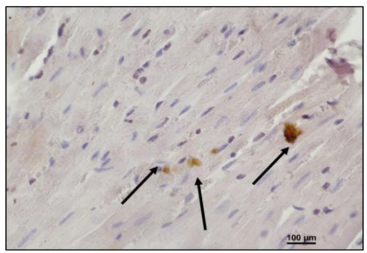
(ii)
100 µm

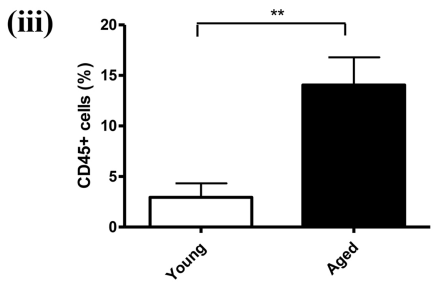
(iii)
**
CD45+ cells (%)
20
15
10
5
0
Young
Aged

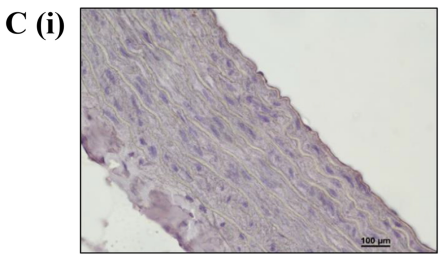
C (i)
100 µm

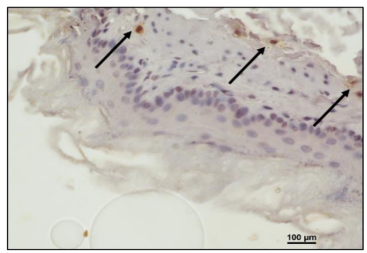
(ii)
100 µm

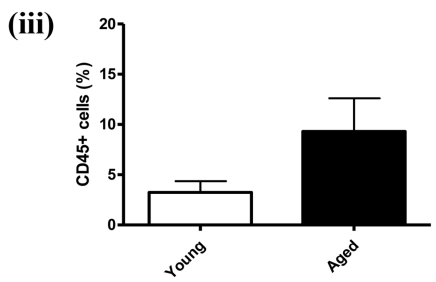
(iii)
CD45+ cells (%)
20
15
10
5
0
Young
Aged

Figure 5

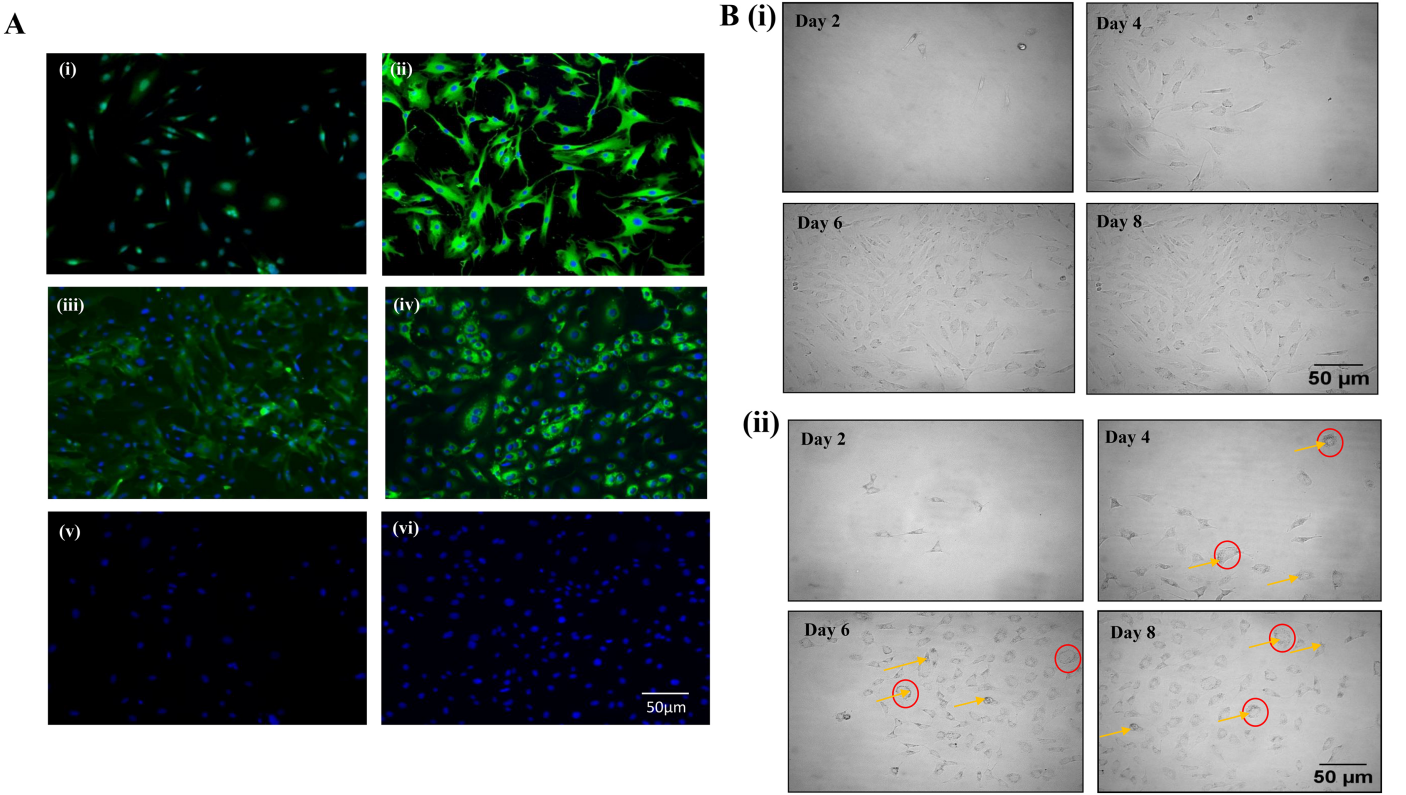
A
(i)
(ii)
(iii)
(iv)
(v)
(vi)
50µm
B (i)
Day 2
Day 4
Day 6
Day 8
50 µm
(ii)
Day 2
Day 4
Day 6
Day 8
50 µm

Figure 6

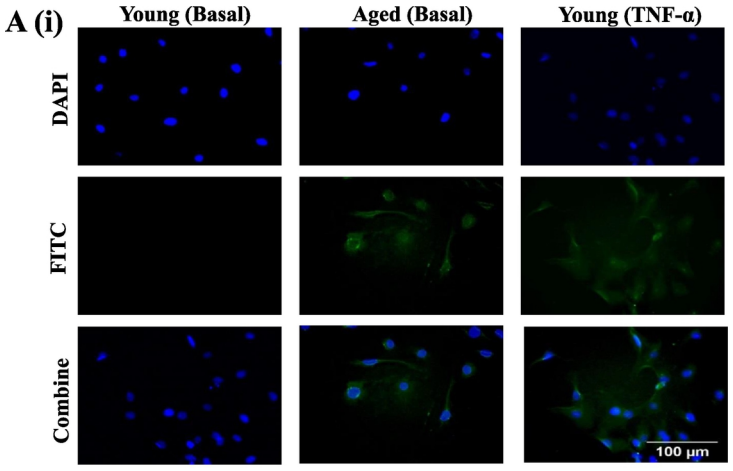
A (i)
Young (Basal)
Aged (Basal)
Young (TNF-α)
DAPI
FITC
Combine
100 μm

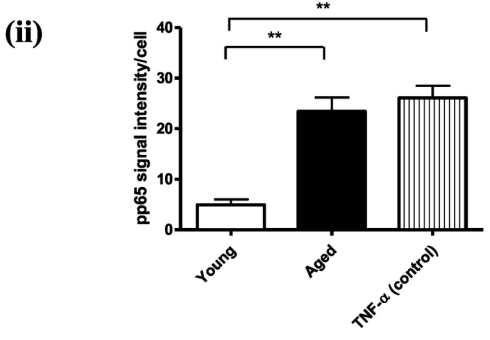
(ii)
pp65 signal intensity/cell
40
30
20
10
0
**
**
Young
Aged
TNF-α (control)

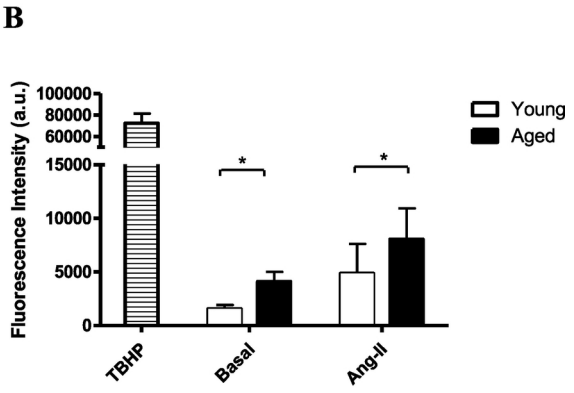
B
Fluorescence Intensity (a.u.)
100000
80000
60000
15000
10000
5000
0
*
*
TBHP
Basal
Ang-II
Young
Aged

Figure 7

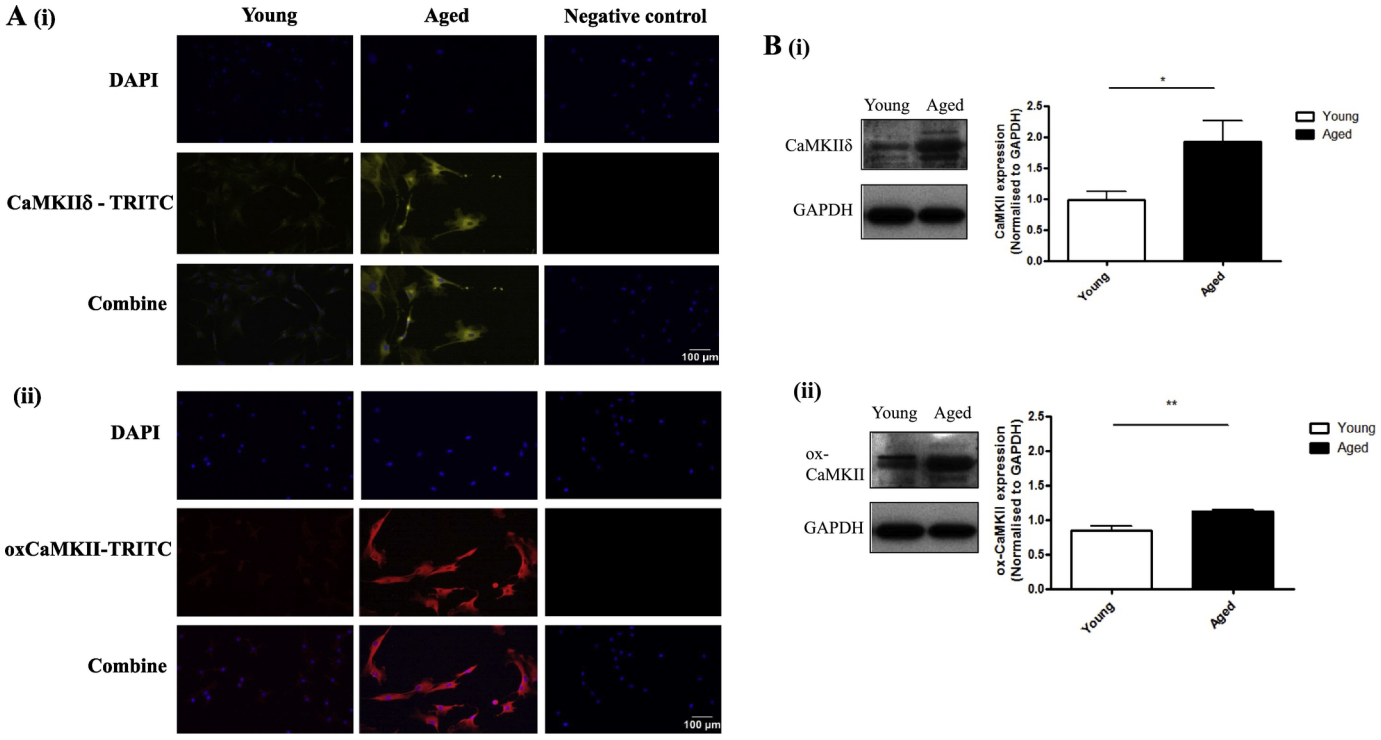
A (i)
Young
Aged
Negative control
DAPI
CaMKIIδ - TRITC
Combine
100 µm
(ii)
DAPI
oxCaMKII-TRITC
Combine
100 µm
B (i)
Young
Aged
CaMKIIδ
GAPDH
*
CaMKII expression (Normalised to GAPDH)
2.5
2.0
1.5
1.0
0.5
0.0
Young
Aged
(ii)
Young
Aged
ox-CaMKII
GAPDH
**
ox-CaMKII expression (Normalised to GAPDH)
2.5
2.0
1.5
1.0
0.5
0.0
Young
Aged

Figure 8